Journal of Fluorescence, Vol. 7, No. 3, 1997

Autoreconvolution—An Extension to the "Reference Convolution" Procedure for the Simultaneous Analysis of Two Fluorescence Decays from One Sample

G. Rumbles,[1,4] T. A. Smith,[2,4] A. J. Brown,[1] M. Carey,[1] and I. Soutar[3]

Received April 2, 1997; accepted August 14, 1997

A fast and simple method of analyzing fluorescence decay data collected using the time-correlated single-photon counting technique is presented. The technique is related to the "reference convolution" method and is applicable to systems characterized by groups of fluorescence decays which are interrelated such that each can be fitted by a sum of exponentials which differs only in preexponential factors from that descriptive of another in the set. Suitable cases include monomer/excimer systems, fluorescence anisotropy decay analysis, and heterogeneous emission systems. The advantages of this method are discussed with examples of its application.

KEY WORDS: Fluorescence decay analysis; reconvolution; reference convolution.

INTRODUCTION

The technique of time-correlated single-photon counting (TCSPC)[1] is a powerful detection tool for studying the photophysics of excited electronic states of molecular species. However, fluorescence decay data collected using this method are distorted by a number of factors inherent in the technique. Perhaps the most serious of these problems is the finite width and substructure of the instrument response function. The standard practice to overcome this difficulty has been to collect a fluorescence decay at the desired emission wavelength and then collect an instrument response function at the excitation wavelength by collecting excitation light scattered from a dilute suspension of a nonfluorescent diffuse scattering solution such as Ludox (colloidal silica) or nondairy whitener.[2] This instrument response function (IRF) is assumed to be identical to the response one would obtain at the experimental emission wavelength used in the experiment and is then used in a deconvolution or reconvolution procedure to recover the desired kinetic parameters. This practice, although convenient, suffers from inherent drawbacks due to (i) the time shift (and possible shape change) of the instrument response profile as a function of wavelength,[3-5] (ii) the count rate dependence of instrument response functions obtained using microchannel plate photomultiplier tubes,[6] (iii) having to change the sample cuvette between sample and scatterer with associated difficulties in certain circumstances (such as temperature-dependent experiments employing bulky cryostats), and (iv) problems with fitting the leading edges of decays

One effective method of overcoming at least some of these problems is the "reference convolution" technique,[7] in which a fluorescence decay, collected from a reference compound, is used instead of an instrument response function in the convolution procedure. The reference convolution method relies on the ability to find a

[1] Chemistry Department, Imperial College of Science, Technology and Medicine, Exhibition Road, London SW7 2AY, U.K.
[2] School of Chemistry, University of Melbourne, Parkville, Australia, 3052.
[3] The Polymer Centre, Lancaster University, Lancaster LA1 4YA, UK
[4] To whom correspondence may be addressed.

1053-0509/97/0900-0217$12.50/0

suitable reference compound, i.e., one which absorbs and fluoresceses at the same wavelengths as the sample under investigation and whose fluorescence decay is exponential. This method still requires the changing of cuvettes and has other associated problems in temperature-dependent studies and other experiments such as time-resolved evanescent wave-induced fluorescence spectroscopy (TREWIFS),[8] in which it is difficult to replace the sample reproducibly with a reference compound.

The convolution of one fluorescence decay with another from the same sample has been attempted only rarely, partly because it was not thought to produce meaningful results. In this paper we discuss the possibility of analyzing some types of fluorescence decay curves using a procedure closely related to the reference convolution method but which involves the iterative reconvolution of two decays collected from the *same* sample, either decays from different wavelength regions (such as in a monomer/excimer system) or decays corresponding to emission with polarization parallel and perpendicular to the polarization of the excitation light in anisotropy experiments. We show that, in certain circumstances, the true fluorescence lifetimes or rotational correlation times can be recovered.

Lakowicz and Balter[9,10] have used a similar approach, called differential-wavelength deconvolution, to analyze fluorescence decays. This method has been used on data collected from a tryptophan derivative in which solvent relaxation effects caused complex fluorescence decay behavior.[9] In that work, the decay collected from the blue side of the emission band, corresponding to fluorescence from the initially excited state, was assumed to follow a single-exponential functional form and was then used in the convolution procedure when analyzing the decays collected at wavelengths more to the red of the emission band, corresponding to emission from the solvent relaxed state. In a second paper,[10] the method was tested on the excited-state protonation of acridine and the excited-state deprotonation of 2-naphthol.

The convolution kinetics approach[11] is another method of fluorescence decay curve analysis which uses the decay profile corresponding to emission from one species (the monomer) in the analysis of another species which emits in another wavelength region (the excimer). The fluorescence decay of the excimer is then assumed to be described by the convolution of the monomer decay with a single-exponential decay. Transient effects, caused by the diffusion-controlled nature of excimer formation, can also be taken into account in this method by including a time-dependent rate coefficient in the convolution function.[12]

A related method for the analysis of fluorescence anisotropy decays is the so-called "impulse reconvolution"[13,14] approach, in which the experimental decays, collected with an emission polarization analyzer set parallel, $I_{\parallel}(t)$, and perpendicular, $I_{\perp}(t)$, to the plane of polarization of the excitation light, are used to generate sum $[I_s(t) = I_{\parallel}(t) + 2 \cdot I_{\perp}(t)]$ and difference $[I_d(t) = I_{\parallel}(t) - I_{\perp}(t)]$ decay profiles. A convenient model function (e.g., a sum of exponentials) is used in iterative reconvolution with the instrument response function to fit the $I_s(t)$ data. The resultant fitting function (the impulse response function) $[I_s(t)]$ is then combined with an appropriate model for the anisotropy function, $r(t)$ (e.g., a single-exponential for an isotropic rotor), and the product $r(t) \cdot I_s(t)$ compared to $I_d(t)$. The fitting parameters within the trial function chosen for $r(t)$ are then adjusted iteratively in a nonlinear minimization procedure to yield the desired relaxation information.

The method, that of autoreconvolution, described in this paper is a little more general than the techniques mentioned above and is applicable to systems in which two fluorescence decays collected from the same sample can be modeled by a sum of exponentials which differ only in preexponential factors, i.e., the decay rate constants are the same for each decay. Each decay must also be represented by the same number of exponential terms in the fitting function. Suitable cases include simple monomer/excimer systems, fluorescence anisotropy decay analysis, and even mixtures of noninteracting chromophores. The autoreconvolution approach is also less susceptible to leading-edge fitting problems and is far more convenient than the standard reference convolution method for temperature-dependent studies and TREWIFS. We consider this method a useful complementary technique to the rigorous method of "second-generation" global analysis, in which many decays (rather than just two) can be analyzed simultaneously, and parameters linked through an assumed mathematical relationship.[15,16]

THEORETICAL BACKGROUND

Fluorescence decay data collected using the TCSPC technique can be distorted significantly by the finite width and substructure of the detection system's response. In such cases the measured decay profiles, $I(t)$, are actually a convolution of the instrumental response function, $P(t)$, with the true fluorescence decay, $F(t)$:

$$I(t) = P(t) \otimes F(t) = \int_0^t P(t') \cdot F(t - t')dt' \quad (1)$$

where $\otimes$ indicates a convolution and t' is a "dummy" time variable.

To derive the true decay profile, $F(t)$, the effect of $P(t)$ must be removed, or deconvolved from $I(t)$, and several methods by which Eq. (1) can be solved have been developed, with varying degrees of success, versatility, and computational complexity. Descriptions and critical comparisons of some of these methods as applied to TCSPC data appear in the literature,[1,17-19] with the most popular method being that of nonlinear least-squares iterative reconvolution (NLLSIR). The popularity of this method is due to its reliability and its ability both to resolve closely spaced decay times and to fit any chosen section of the decay curve with no loss of accuracy. In the NLLSIR method, the detection system's measured intensity–time profile (IRF), $P(t)$, is not first *de*convoluted from the measured decay but is, instead, convoluted with the trial function chosen for the excited-state decay, $F(t)$. The resultant profile is then compared to the measured experimental decay curve, $I(t)$. This convolution fitting procedure is repeated by adjusting the parameters in such a way as to minimize (usually using the Levenburg–Marquardt algorithm[20,21]) the value of the reduced chi square, χ_r^2, defined as the weighted sum of the squares of the deviations of the experimental points from the calculated fitting function.

$$\chi_r^2 = \frac{\sum_{i=n_1}^{n_2} w_i^2 \left[I(t_i) - F(t_i)\right]^2}{n_2 - n_1 + 1 - p} \qquad (2)$$

In Eq. (2), n_1 and n_2 are the first and last channels of the section of the decay to be analyzed with p adjustable parameters. w_i is the weighting factor of channel i, which, since photon counting error is Poisson-distributed,[22-24] is given by $w_i = 1/\sqrt{I(t_i)}$.

An element of uncertainty accompanies the traditional NLLSIR method: it is assumed that the wavelength dependence of the instrument response function, $P(t, \lambda)$, can be reduced to negligible proportions. $P(t, \lambda)$ is a composite entity encompassing the excitation pulse profile, $E(t, \lambda)$, the photomultiplier response, $D(t, \lambda)$, and the response of the remaining TCSPC electronics, $K(t)$. The general practice is to assume that the wavelength dependence of $D(t, \lambda)$ is greater than that of $E(t, \lambda)$ and the excitation prompt, $P(t, \lambda_{em})$, recorded at the emission wavelength chosen for analysis of the fluorescence is taken to represent $P(t)$ in the reconvolution procedure. This is straightforward with flashlamp or synchrotron excitation sources but the limited tunability of pulsed lasers can pose problems. In the latter instance it is customary to use $P(t, \lambda_{ex})$, recorded at the excitation wavelength, to represent $P(t)$.

In most cases, the validity of the assumption $P(t, \lambda_{ex}) = P(t, \lambda_{em})$ is questionable due to the well-known wavelength dependence of the temporal position and shape of instrument response functions obtained with most photomultiplier tubes.[3-5] While this effect is reportedly less prevalent for microchannel plate photomultipliers,[25] it does still occur and other problems (such as count rate dependence)[6] are often encountered. Furthermore, curve fitting over the entire time range of a decay curve is often difficult, especially when using microchannel plate (MCP) photomultiplier tubes, the rise time of which is often very fast when long decay times (>300 ps) are recorded. The Grinvald and Steinberg[22] approximation assumes that the histogram IRF is a good representation of the true IRF, however, with fast-rise time IRFs, this is not always the case and the shift parameter often does not work properly. The ability of the autoreconvolution method to overcome these problems is one of its most attractive features.

The reference convolution method has, in recent years, gained popularity due to its success in overcoming some of the problems mentioned above regarding the standard iterative reconvolution procedure with an instrument response function. It has even been used successfully in association with global analysis techniques.[7] In the reference convolution method, the trial function for the excited-state decay is assumed to be a sum of n exponential terms and the fluorescence decay from a reference compound is used in the iterative reconvolution procedure in place of the IRF. The fluorescence decay of the reference compound, $I_r(t, \lambda_{em})$, *must* be known to follow a single-exponential function (which is not always easy to prove on short time scales) with decay constant k_r, and furthermore, k_r must not be equal to any of the rate constants in the trial function (i.e., $k_r \neq k_i$). The observed fluorescence decay profiles are then given by Eqs. (3) and (4).

$$I(t, \lambda_{em}) = P(t) \otimes \sum_{i=1}^{n} A_i \exp\left[-k_i t\right] \qquad (3)$$

$$I_r(t, \lambda_{em}) = P(t) \otimes A_r \exp\left[-k_r t\right] \qquad (4)$$

By taking the ratio of the Laplace transforms of these equations, the IRF term can be removed from the problem and the rate coefficients of interest, k_i, can be recovered successfully by fitting the resulting function[7] [Eq. (5)] to the experimental data.

$$I(t, \lambda_{em}) = I_r(t, \lambda_{em}) \sum_{i=1}^{n} A_i + I_r(t, \lambda_{em}) \left\{ \sum_{i=1}^{n} A_i (k_r - k_i) \cdot \exp(-k_i t) \right\} \quad (5)$$

The situation under discussion in this paper is when two decays, $I_1(t)$ and $I_2(t)$, are collected from the same sample, either decays from different wavelength regions (λ_{em_1} and λ_{em_2}, such as in a monomer/excimer system) or decays corresponding to emission with polarization oriented in planes parallel ($\parallel$) and perpendicular ($\perp$) to the polarization of that of the polarized excitation light, in anisotropy work. This method is valid solely for systems in which fluorescence decays can be fitted by a sum of exponentials which differ only in the magnitude of the preexponential factors, i.e., all lifetimes are the same, and each decay is represented by the same number of exponential terms in the fitting function. The two measured fluorescence decays can then be summarized by Eqs. (6) and (7).

$$I_1(t, \lambda_{em_1} \text{ or } \parallel) = \int_0^t P(t') \cdot F_1(t - t')\, dt' \quad (6)$$

$$= P(t) \otimes \sum_{i=1}^{n} A_i \exp[-k_i t]$$

$$I_2(t, \lambda_{em_2} \text{ or } \perp) = \int_0^t P(t') \cdot F_2(t - t')\, dt' \quad (7)$$

$$= P(t) \otimes \sum_{i=1}^{n} B_i \exp[-k_i t]$$

Taking the Laplace transforms of Eqs. (6) and (7) reduces the convolution to a simple multiplication, giving

$$\mathbf{L}[I_1(t)] = \mathbf{L}[P(t, \lambda_{em})] \cdot \sum_{i=1}^{n} \left[\frac{A_i}{s + k_i} \right] \quad (8)$$

$$\mathbf{L}[I_2(t)] = \mathbf{L}[P(t, \lambda_{em})] \cdot \sum_{i=1}^{n} \left[\frac{B_i}{s + k_i} \right] \quad (9)$$

where $\mathbf{L}$ represents the Laplace transform operator and s is the Laplace transform variable of t. Division of Eq. (9) by Eq. (8) removes the $\mathbf{L}[P(t, \lambda_{em})]$ term, and after rearrangement the problem becomes one of either (i) finding the inverse Laplace transform of the right-hand side of Eq. (10) or (ii) predicting a solution, taking its Laplace transform, and equating this with the right-hand-side of Eq. (10).

$$\frac{\mathbf{L}[I_2(t)]}{\mathbf{L}[I_1(t)]} = \sum_{j=1}^{n} \frac{B_i}{(s + k_j) \cdot \sum_{i=1}^{n} [A_i/(s + k_i)]} \quad (10)$$

Adopting the second of these methods, and by analogy with the solution in Löfroth's paper,[7] a trial function for the solution of this problem is one of the form $\mathbf{L}[G(t)] + \alpha$, and it has been found empirically (see Appendix) that Eq. (11) is a satisfactory solution for $G[(t)]$.

$$G(t) = \sum_{i=1}^{n-1} \beta_i \exp(-\gamma_i t) \quad (11)$$

Summarizing Eq. (11), if two decays which conform to the criteria discussed above are analyzed using this technique (i.e., where one decay is used in place of the IRF), the analytical function required to fit the data would be of the form $\sum_{i=1}^{n-1} \beta_i \exp(-\gamma, t) + \alpha$ [i.e., it would consist of a constant term, α, plus a sum of exponentials with one fewer exponential term than would be the case if the conventional method (iterative reconvolution with an IRF) was used on each decay individually]. While in principle this procedure is applicable for any value of n, bi- and triexponential functions represent the vast majority of common experimental situations. Consequently, we have concerned ourselves in this paper only with situations where $n \leq 3$. In any case, meaningful interpretation of results from the use of multiexponential functions with $n > 3$ is often difficult and the validity of the use of such functions is questionable. Furthermore, the association of the parameters recovered from the analysis method under discussion here, β_i and γ_i, with the "true" decay parameters, A_i and τ_i, for $n > 3$ is extremely complex and difficult to justify. This, however, does not detract from the success of this method for cases of $n \leq 3$.

In order to associate the parameters obtained from this method with the "true" decay parameters, Eq. (12) must be solved:

$$\mathbf{L}[G(t)] + \alpha \Rightarrow \sum_{i=1}^{n-1} \left(\frac{\beta_i}{s + \gamma_i} \right) + \alpha = \sum_{j=1}^{n} \frac{B_i}{(s + k_j) \cdot \sum_{i=1}^{n} [A_i/(s + k_i)]} \quad (12)$$

The solutions to Eq. (12) are derived in the Appendix for the specific cases of $n = 2$ and $n = 3$. While the approach shown is not mathematically rigorous, a pattern for the β_i and γ_i terms is recognizable as n increases, and a generalization of this pattern which is simple to write down is being sought. The term for α, however, can be generalized as given in the Appendix. This parameter can be included as a scattered light or

variable baseline term in many existing iterative reconvolution software packages.

In the following sections we examine these relationships in some detail and present results obtained using this technique to analyze fluorescence decay data simulated to mimic anisotropy decay data, monomer/excimer systems, and triple-exponential decays. We have also had considerable success using this method on data from real monomer/excimer[26] and anisotropy decay[27] systems. We compare these results with those obtained using the conventional (iterative reconvolution procedure with an IRF) method and discuss in detail the advantages and limitations of the autoreconvolution approach.

RESULTS AND DISCUSSION

Decay curves were generated by convolving various sums-of-exponential functions, $F(t)$ (as detailed below), with experimentally recorded instrument response profiles of various time calibration factors, using the convolution integral [Eqs. (6) and (7)]. Computer-generated Poissonian noise was then added to the resultant decay curves in order to provide suitable statistics for the fitting routines.[1] The decay constants used in the simulation of the decay curves were chosen to mimic typical experimental situations such as fluorescence anisotropy and monomer/excimer systems. Examples are quoted where simple kinetics apply and in which the method can be used to demonstrate the plausibility of the resulting "fitting function(s)." In other cases we demonstrate how the technique can show that the assumed kinetic solution is invalid.

Fluorescence Anisotropy Analysis

Time-resolved fluorescence anisotropy measurements involve the measurement of the observed fluorescence intensity profiles, $I_\parallel(t)$ and $I_\perp(t)$, detected, at right angles to the direction of vertically polarized excitation using a polarizing analyzer element, aligned in a parallel and perpendicular orientation, respectively, to the polarization vector of the exciting radiation. Following excitation using a delta-function, the parallel and perpendicular fluorescence intensity components for a chromophore exhibiting a single-exponential fluorescence decay and undergoing an idealized first-order rotational reorientation process would decay according to Eqs. (13) and (14), respectively, in which k_f is the first-order rate constant for the total fluorescence decay ($= 1/\tau_f$, where τ_f is the fluorescence lifetime), k_r is the rate constant governing the rotational relaxation of the chromophore ($= 1/\tau_r$, where τ_r is the rotational correlation lifetime), and r_0 is the "intrinsic anisotropy" observed in the absence of rotational relaxation.

$$I_\parallel(t) = e^{-k_f t}(1 + 2r_0 e^{-k_r t}) = e^{-k_f t} + 2r_0 e^{-(k_f + k_r)t} \quad (13)$$

$$I_\perp(t) = e^{-k_f t}(1 - r_0 e^{-k_r t}) = e^{-k_f t} - r_0 e^{-(k_f + k_r)t} \quad (14)$$

The time-dependent emission anisotropy, $r(t)$, is given by Eq. (15) and, in the simple case under discussion here, is related to the rotational correlation time by Eq. (16).

$$r(t) = \frac{I_\parallel(t) - I_\perp(t)}{I_\parallel(t) + 2I_\perp(t)} \quad (15)$$

$$r(t) = r_0 e^{-k_r t} \quad (16)$$

The various methods of extracting τ_r values from fluorescence anisotropy data and the advantages and drawbacks of these techniques have been discussed in detail elsewhere.[28,29] Suffice it to say that there are numerous problems associated with most methods of analysis, and an alternative, reliable method is required. The pair of Eqs. (13) and (14) conforms to the requirements of the autoreconvolution technique discussed above, namely, they involve the same number of exponential terms ($n = 2$) with the same two rate constants, k_f and $(k_r + k_f)$, and only the preexponential factors differing, and so it is an ideal candidate for investigation via this technique.

Decays intended to mimic typical fluorescence anisotropy data obtained from a small rotor were generated using Eqs. (13) and (14). The values used for r_0, k_r, and k_f in the simulation are summarized in Table I. The resulting $I_\parallel(t)$ and $I_\perp(t)$ decays were normalized appropriately prior to the artificial noise being added and assuming the instrumental "G factor" to be unity. Figure 1 shows the simulated decay profiles and the best fit resulting from a single-exponential autoreconvolution analysis of the $I_\perp(t)$ data using Eq. (17).

$$I_\perp(t) = \int_0^t I_1(t) \cdot \beta \cdot \exp(-\gamma(t - t'))dt' + \alpha I_1(t) \quad (17)$$

In this procedure $I_\parallel(t)$ is used along with an appropriate trial function in an iterative reconvolution of $I_{=\kappa}(t)$ in which $I_\parallel(t)$ adopts a role analogous to that of the IRF in fitting an observed fluorescence profile, $I(t)$, contaminated with scattered light [the $\alpha I_\parallel(t)$ term in Eq. (17) being analogous to the "scatter correction term," $cP(t)$, which would be incorporated into the latter type of "fit"]. The results obtained from this analysis are summarized in Table I.

Table I. Parameters Used and Recovered in the Test of the Method on Simulated Anisotropy Data[a]

Value used in simulation using Eqs. (13) & (14)	Predicted value	Recovered value for parameter using $I(t) = \beta \exp(-\gamma t) + \alpha$	Parameter calculated from recovered value and using Eqs. (18) & (19)
$r_o = 0.4$ $k_1 = 1.18$ (ns^{-1})	$\alpha = 0.3333$ $\gamma = 2.10$ (ns^{-1})	$\alpha = 0.327$ $\gamma = 2.10$ (ns^{-1})	$r_o = 0.406$ $k_r = 1.667$ (ns^{-1}) assuming $k_f = 1.18$ (ns^{-1})
$k_2 = (1/\tau_f) + (1/\tau_r) = 2.84$ (ns^{-1}) [where $1/\tau_r = 1.66$ (ns^{-1})]			

[a]Decay curves were simulated according to Eqs. (13) and (14) (where $k_1 = k_f$, $k_2 = k_f + k_r$) and normalized according to $A_1 = 50{,}000$ (counts), $A_2 = 40{,}000$ (counts), $B_1 = 50{,}000$ (counts), and $B_2 = -20{,}000$ (counts).

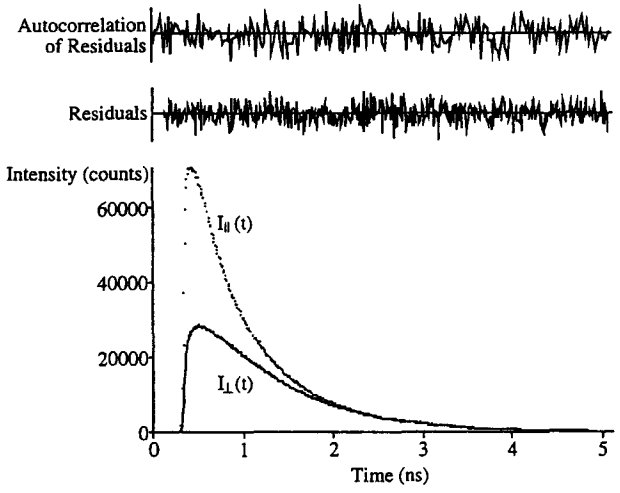

Fig. 1. Simulated parallel, $I_{\parallel}(t)$, and perpendicular, $I_{\perp}(t)$, decays for anisotropy analysis. The solid line is the resultant best fit to $I_{\perp}(t)$ using autoreconvolution with $I_{\parallel}(t)$ in place of the IRF, as summarized in Table I.

Equations (A5) and (A6) derived in the Appendix can be readily transformed to give expressions (18) and (19) specific to the case in point, from which values for r_0 and τ_r ($= 1/k_r$) can be calculated if τ_f ($= 1/k_f$) is known from an independent experiment (e.g., from analysis of the magic angle decay) or from analysis of the sum decay, $I_s(t)$.

$$\alpha = \frac{(1 - r_0)G}{1 + 2r_0} \tag{18}$$

$$\gamma = \frac{k_f + k_r + 2r_0 k_f}{1 + 2r_0} \tag{19}$$

When A_1, A_2, B_1, and B_2 are related, it is possible to use the values of α and β. When no relationship exists, i.e., two arbitrary decays, then only the γ term carries useful information. In the case presented here, $G = 1$ and the decays tail match, thus indicating that there is indeed a relationship among A_1, A_2, B_1, and B_2.

It is apparent from the details shown in Table I that the predicted values are in fact recovered. It is particularly pleasing to note the ability of the technique to recover the correct r_0 value directly from a single fitting parameter. This technique has been used with success recently on experimental anisotropy data obtained from fluorophore-labeled polymers in dilute solution,[27] where it compared favorably with the impulse reconvolution procedure.

In the case of anisotropy data, the IRF is the same in both cases, and therefore the autoreconvolution method is ideal. It is also possible to reverse the analysis, i.e., analyze $I_{\parallel}(t)$ using $I_{\perp}(t)$ as the "response function" in the autoreconvolution procedure, and the method still works. However, the interpretations of Eqs. (A5) and (A6) will differ from Eqs. (18) and (19).

Analysis of Monomer/Excimer Systems

A further example of the usefulness of this method of analysis is the case of monomer/excimer systems. In this section we consider three common situations that can arise in such systems. First, we consider an ideal monomer/excimer system that follows Birks' kinetic scheme.[30] Second, we consider the case where a rate parameter in the monomer decay does not quite correspond to either rate parameter in the excimer decay. This illustrates the power of this analysis method in determining whether or not a simple kinetic scheme is appropriate. Finally, we consider the case in which the two preexponential factors of the excimer decay are not equal and opposite as predicted by Birks' kinetic scheme. These circumstances are common in cases where fluorescence decays are collected from synthetic aromatic polymers and their model compounds.[31-33]

Table IIa. Parameters Used and Recovered in the Test of the Method on Simulated Monomer/Excimer Data for the Case of Ideal Birks' Kinetics[a]

Value used in simulation using eqs. (20) & (21)	Predicted value for parameter using $I(t) = \beta\exp(-\gamma t) + \alpha$	Recovered value for parameter using $I(t) = \beta\exp(-\gamma t) + \alpha$
$k_1 = 1.57 \times 10^8$ (s^{-1})	$\alpha = 0.0$	$\alpha = 0.0$
$k_2 = 4.37 \times 10^7$ (s^{-1})	$\gamma = 0.05476$ (ns^{-1})	$\gamma = (1/18.28) = 0.05470$ (ns^{-1})
		$\beta = 0.044$

[a]Simulated curves were normalized according to $A_1 = 46{,}000$ (counts), $A_2 = 5000$ (counts), $B_1 = -100{,}000$ (counts), and $B_2 = 100{,}000$ (counts).

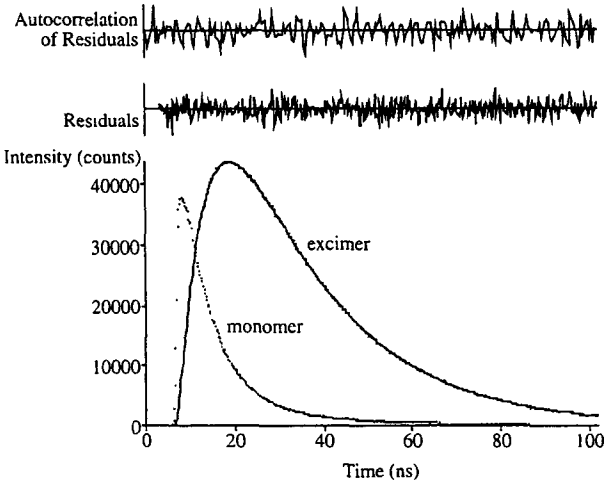

Fig. 2. Simulated monomer, $I_m(t)$, and excimer, $I_e(t)$, decays for the case of perfect Birks' kinetics [refer to Eqs. (19) and (20)]. The solid line is the resultant best fit to $I_e(t)$ using autoreconvolution with $I_m(t)$ in place of the IRF, as summarized in Table IIa.

Simple Kinetic Scheme

In monomer/excimer systems, an ideal system is one which follows the kinetic scheme proposed by Birks *et al.*,[30] in which the monomer, $I_m(t)$, and excimer, $I_e(t)$, decay profiles are predicted to be described by Eqs. (20) and (21), respectively:

$$I_m(t) = A_1 \cdot \exp(-k_1 t) + A_2 \cdot \exp(-k_2 t) \quad (20)$$

$$I_e(t) = B_1 \cdot \exp(-k_1 t) - B_2 \cdot \exp(-k_2 t) \quad (21)$$

where the k's, A's, and B's consist of combinations of the various rate constants in the reaction scheme.[30] Of course in the case of Birks' kinetics, $B_1 = B_2$, since no excimers exist at $t = 0$. In order to test the method under discussion here, two decay curves were synthesized as above using the parameters given in Table IIa and analyzed with a standard NLLSIR program using the monomer decay in place of the instrument response function. As predicted by Eq. (11), a single-exponential function was required to fit the data satisfactorily (Fig. 2). The values obtained for α, β, and γ from this analysis are also given in Table IIa. Again, from Eqs. (A5) and (A6), terms in α, β, and γ can be expressed as in Eqs. (22)–(24), from which it can be seen that in a system which follows Birks' kinetic scheme perfectly (i.e., $B_1 = B_2$), α should equal zero when the autoreconvolution is carried out using the monomer decay in place of the IRF.[5]

$$\alpha = \frac{B_1 - B_2}{A_1 + A_2} \quad (22)$$

$$\gamma = \frac{A_1 k_2 + A_2 k_1}{A_1 + A_2} \quad (23)$$

$$\beta + \alpha\gamma = \frac{B_1 k_2 - B_2 k_1}{A_1 + A_2} \quad (24)$$

It should be noted that, unlike the anisotropy case, in which the the number of excitation photons incident on the sample is attempted to be kept the same for the two decays through some form of excitation intensity integrator, polarizer "toggling," or use of T-geometry (with matched detectors), monomer/excimer decay pairs are often collected to the same number of counts in the channel of the maximum intensity or for the same collection time. This means that there is usually no fixed scaling factor between the preexponential factors A and B, and so the α and β terms [Eqs. (22) and (24)] provide no useful information in this case.

While deriving values for the two rate parameters k_1 and k_2 relies on knowledge of the preexponential factors A_1, A_2, and B_1 ($=|B_2|$), the technique can obviously be used to verify the applicability of Birks'-type kinetic scheme, merely from the value of α, which should equal zero for the present case as mentioned above. It is, in fact, because $\alpha = 0$ that the derivation of values for k_1

[5] Compare this with the opposite case, i.e., when the excimer decay is used in place of the IRF, in which case $\alpha \to \infty$ and computational problems will arise.

Table IIb. Parameters Used and Recovered in the Test of the Method on Simulated Monomer/Excimer Data for the Case of Nonideal Birks' Kinetics Where the Rate Parameters Are Not Consistent Between the Monomer and the Excimer Decays[a]

Value used in simulation	Predicted and recovered values for parameters using $I(t) = \beta_1\exp(-\gamma_1 t) + \beta_2\exp(-\gamma_2 t) + \alpha$	
$k_{m_1} = 1.57 \times 10^8$ (s^{-1})	$\alpha = 0.0$	$\alpha = 0.0$
$k_{m_2} = 5.48 \times 10^7$ (s^{-1})	$\gamma_1 = 6.48 \times 10^7$ (s^{-1})	$\gamma_1 = (1/15.2) = 6.58 \times 10^7$ (s^{-1})
$k_{e_1} = k_{m_1}$	$\gamma_2 = 4.38 \times 10^7$ (s^{-1})	$\gamma_2 = (1/22.7) = 4.41 \times 10^7$ (s^{-1})
$k_{e_2} = 4.38 \times 10^7$ (s^{-1})	$\beta_1 = 1.06 \times 10^{8b}$	$\beta_1 = 0.0223$
	$\beta_1 = 1.16 \times 10^{8b}$	$\beta_1 = 0.0278$

[a]Simulated curves were normalized according to $A_1 = 46{,}000$ (counts), $A_2 = 5000$ (counts), $B_1 = -100{,}000$ (counts), and $B_2 = 100{,}000$ (counts).
[b]Obtained numerically.

and k_2 is so problematic. If the preexponential factors are known from individual analyses of the monomer and excimer curves, then more reliable estimates of the rate parameters can be obtained from autoreconvolution since this technique is analogous to "global analysis" in that both decays are being used simultaneously in the analysis. Autoconvolution is, therefore, a useful complementary technique to other analysis methods, in addition to being able quickly to identify whether Birks' kinetic scheme is valid for a given system.

Non-Birks' Kinetics

Situations in which fluorescence decays can be fitted satisfactorily by the simple scheme summarized by Eqs. (17) and (18) have proven to be extremely rare, especially in the field of synthetic aromatic polymers and their model compounds. Often, more complicated decay fitting functions requiring sums of more than two exponential terms are required. Commonly even when double-exponential functions are adequate, discrepancies exist between the rate parameters recovered from individual analyses of decays collected from the monomer and excimer spectral regions, i.e., $k_{m_1} \neq k_{e_1}$ or $k_{m_2} \neq k_{e_2}$, or even more commonly, the preexponential factors of the decay function for the excimer analysis [Eq. (20)] are not equal and opposite in sign. Here we address these two cases and show that autoreconvolution provides a quick and convenient method of checking the validity of Birks' kinetic scheme to a particular system.

The Case where $k_{m_1} \neq k_{e_1}$ (or $k_{m_2} \neq k_{e_2}$). If one of the rate parameters is not consistent between the two analysis functions [Eqs. (19) and (20)], one of the restrictions inherent in the autoreconvolution technique is violated, which we should be able to identify. To illustrate this, two decay curves were synthesized as above using the parameters given in Table IIb and analyzed in the same way as in Simple Kinetic Scheme (above). In contrast to the case of ideal Birks' kinetics discussed above, a single-exponential function was inadequate to fit the data satisfactorily (based on the usual goodness-of-fit criteria, e.g., $\chi^2 = 3.648$, Durbin–Watson parameter = 0.484; see plots of weighted residuals and autocorrelation in Fig. 3a), but a double-exponential function is shown to be adequate (Fig. 3b). This would be expected, as it is a trivial case of three common decay times with some preexponential factors being zero (see Triple-Exponential Analysis, below). The entries for β_1 and β_2 in column 2 of Table IIb are obtained numerically, whereas those in column 3 are those returned from the analysis. The difference in the β_1:β_2 ratios of the entries in column 2 compared with those in column 3 further indicates the failure of the method when the inherent assumptions of the technique are invalid. In the context of the discussion here, this analysis serves no useful function other than illustrating the power of the autoreconvolution technique to discriminate between cases of Birks' kinetics and cases when the kinetic model breaks down.

The Case where $B_1 \neq B_2$. The other common violation of Birks' kinetic scheme is where the preexponential factors in the decay function for the excimer region [Eq. (20)] are not equal and opposite, i.e., $B_1 \neq B_2$. To illustrate this, two decay curves were synthesized using the parameters given in Table IIc and analyzed as above. A single-exponential function, with the parameters given in Table IIc, was adequate in this case ($\chi^2 = 0.97$, DW = 1.973; plot not shown), however, the α parameter did not equal zero. This behavior is as predicted from Eq. (11) we have not violated any of the inherent assumptions of the autoreconvolution technique, only the predictions of Birks' kinetic scheme, and

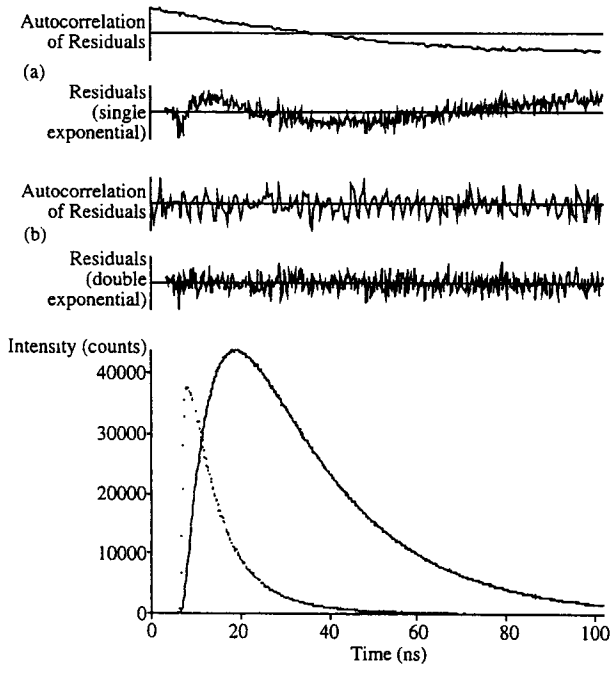

Fig. 3. Simulated monomer, $I_m(t)$, and excimer, $I_e(t)$, decays for the case of non-Birks' kinetic behavior where the rate parameters are inconsistent between the two decays. Two sets of weighted residuals and autocorrelation plots are shown for the case of (a) a single-exponential analysis function and (b) a double-exponential analysis function. The solid line is the resultant best fit using the double-exponential autoreconvolution with $I_m(t)$ in place of the IRF, as summarized in Table IIb.

from Eq. (A5) the magnitude of α is predicted to be proportional to the difference between $|B_1|$ and $|B_2|$.

The examples given above illustrate the power of the autoreconvolution technique in discrimination between the various situations commonly encountered in the study of monomer/excimer systems that can be difficult to resolve from individual analysis of either the monomer or the excimer decay.

Triple-Exponential Analysis

Time-resolved fluorescence decays observed from many systems cannot be analysed on the basis of double-exponential functions. For example, fluorescence decays from the monomer and excimer emission regions of many synthetic aromatic polymer systems have required sums of three, four, or even five exponential terms. Even systems in which the fluorescence decay behavior might intuitively be expected to be less complicated such as bichromophoric molecules[34] have required triple-exponential functions to describe the decays adequately as a function of the emission wavelength across the monomer and excimer regions. In such cases global analysis of all the decays is considered mandatory since, if monomer and excimer decays are analyzed individually, it is often difficult to correlate decay constants between the two regions. The autoconvolution technique provides a quick and independent method for the simultaneous analysis of decays from the two emission regions to determine whether a model based on three common decay constants is appropriate [Eqs. (25) and (26)].

$$I_1(t) = \sum_{i=1}^{3} A_i \exp(-k_i t) \tag{25}$$

$$I_2(t) = \sum_{i=1}^{3} B_i \exp(-k_i t) \tag{26}$$

Extending the test of the autoreconvolution method to the $n = 3$ case, two triple-exponential decays were generated according to Eqs. (24) and (25). The parameters used are summarized in Table III, and were chosen in order to mimic the parameters observed from a typical system. In this case, the curve with the shorter overall decay was used in place of the IRF in the iterative reconvolution of the longer decay. As predicted from Eq. (11), a double-exponential function and associated "α term" were required to fit the data (Fig. 4). The resultant parameters are also reported in Table III. The analytical forms of α, γ_1, and γ_2 are given in the Appendix. The analytical forms for β_1 and β_2 could also be written but are too unwieldy. However, by putting the obtained numerical values of α, γ_1, γ_2, A_i, and k_i into Eq. (A15), two simple equations can be solved to obtain β_1 and β_2 (see Table III, in which it is seen that the ratio of the predicted β values is the same as the β ratio obtained experimentally, unlike the case summarized in Table IIb).

CONCLUSIONS

We have shown here that if two fluorescence decays are measured that can be described by functional forms given by Eqs. (6) and (7), then one decay can be used in the iterative reconvolution analysis procedure in place of an instrument response function. The procedure described, termed "autoreconvolution," which reduces to the case of "reference convolution"[7] when one decay is given by Eq. (4), is not as restrictive as the latter technique. It is shown here that for few enough exponential terms in the fitting function, physically meaningful parameters can still be recovered, and the IRF can be dispensed with. With the exception of when $\Sigma B_i = 0$, the order of the convolution does not matter, i.e.,

Table IIc. Parameters Used and Recovered in the Test of the Method on Simulated Monomer/Excimer Data for the Case of Nonideal Birks' Kinetics Where the Rate Parameters Are Consistent Between the Monomer and the Excimer Decays, but the Preexponential Factors in the Excimer Decay Are Not Equal and Opposite[a]

Value used in simulation	Predicted and recovered values for parameters using $I(t) = \beta \exp(-\gamma t) + \alpha$	
$k_1 = 1.57 \times 10^8$ (s^{-1})	$\alpha = 0.216$	$\alpha = 0.172$
$k_2 = 4.37 \times 10^7$ (s^{-1})	$\gamma = 0.0548$ (ns^{-1})	$\gamma = (1/18.9) = 0.0546$ (ns^{-1})
		$\beta = 0.0443$

[a]Simulated curves were normalized according to $A_1 = 46{,}000$ (counts), $A_2 = 5000$ (counts), $B_1 = -90{,}000$ (counts), and $B_2 = 101{,}000$ (counts).

Table III. Parameters Used and Recovered in the Test of the Method on Simulated Triple-Exponential Decay Data[a]

Value used in simulation	Predicted and recovered values for parameters using $I(t) = \beta_1 \exp(-\gamma_1 t) + \beta_2 \exp(-\gamma_2 t) + \alpha$	
$k_1 = 1.0 \times 10^{10}$ (s^{-1})	$\alpha = 0.3506$	$\alpha = 0.3452$
$k_2 = 3.33 \times 10^9$ (s^{-1})	$\gamma_1 = 3.876$ (ns^{-1})	$\gamma_1 = (1/0.257) = 3.891$ (ns^{-1})
$k_3 = 1.11 \times 10^9$ (s^{-1})	$\gamma_2 = 1.203$ (ns^{-1})	$\gamma_2 = (1/0.826) = 1.210$ (ns^{-1})
	$\beta_1 = 9.96 \times 10^{8}$[b]	$\beta_1 = 0.0040$
	$\beta_2 = 3.98 \times 10^{8}$[b]	$\beta_2 = 0.0016$

[a]Simulated curves were normalized according to $A_1 = 140{,}000$ (counts), $A_2 = 12{,}000$ (counts), $A_3 = 2000$ (counts), $B_1 = 20{,}000$ (counts), $B_2 = 24{,}000$ (counts), and $B_3 = 10{,}000$ (counts).
[b]Obtained numerically.

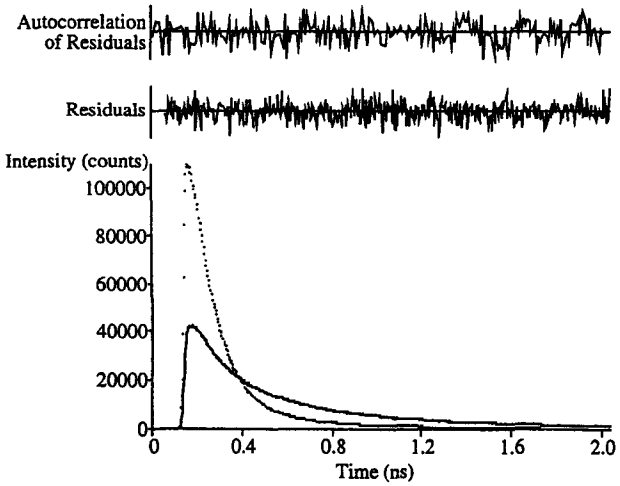

Fig. 4. Simulated triple-exponential decays [Eqs. (24) and (25)]. The solid line is the resultant best fit using a double-exponential autoreconvolution with the shorter-lived decay in place of the IRF, as summarized in Table III.

either decay can be used in place of the IRF. However, it should be noted that the constants α, γ, and α are different in each case. For the simplest cases, such as the fluorescence anisotropy and Birks' kinetics examples given, the individual parameters can be evaluated with a high accuracy. In fact, this technique has been used successfully on real fluorescence anisotropy data as reported previously.[27] In the more complicated systems (e.g., $n = 3$, or where Birks' kinetic scheme is not valid), the autoreconvolution technique is limited to confirming whether the underlying assumption that the two decays can be described by functions with the same number of terms and with the same decay constants is valid. This makes the technique a very useful complementary analysis method in complex systems.

The method described has the following additional advantages. It is related to global analysis in that both decays are analyzed simultaneously and the parameters are therefore linked. It utilizes existing iterative reconvolution software[6] and involves fewer fitting parameters than analysis of decays individually. In addition, it has

[6] Provided that the software does not normalize the IRF (decay) as some programs do in order to calculate the preexponential factors in units of counts.

proven to be far more immune to leading-edge fitting problems than many other analysis techniques. It is useful for experimental situations where reliable instrument response functions can be difficult to record, such as in temperature-dependent work, time-resolved evanescent wave-induced fluorescence measurements, and ultrafast pump-probe studies such as transmission or fluorescence upconversion. While this method cannot be considered a replacement for existing analysis methods, it has been found to be extremely useful for certain situations and as a complementary method in some other cases.

APPENDIX: DERIVATION OF A SOLUTION TO EQ. (10)

Adopting the method of predicting a solution to Eq. (10), taking its Laplace transform, and equating with the right-hand side of Eq. (10), we use the analogy with the solution in Löfroth's paper[7] and employ a trial function of the form $\mathbf{L}[G(t)] + \alpha$, with $G(t)$ taking the form

$$G(t) = \sum_{i=1}^{n-1} \beta_i \exp(-\gamma_i t) \tag{A1}$$

Now, taking the Laplace transform of $G(t)$ and equating with the right-hand side of Eq. (10), the problem becomes one of solving A2.

$$\begin{aligned} L[G(t)] + \alpha &= L\left[\sum_{i=1}^{n-1} \beta_i \exp(-\gamma_i t)\right] + \alpha \\ &= \sum_{i=1}^{n-1} \left[\frac{\beta_i}{s + \gamma_i}\right] \\ &= \frac{\sum_{j=1}^{n} [B_j/(s + k_j)]}{\sum_{j=1}^{n} [A_j/(s + k_j)]} \end{aligned} \tag{A2}$$

As discussed in the text, the majority of real experimental situations is concerned with cases where $n \leq 3$, so here we derive expressions only for $n = 2$ and $n = 3$.

$n = 2$

From Eq. (A2),

$$\frac{\beta}{s + \gamma} + \alpha = \frac{s(B_2 + B_2) + B_1 k_2 + B_2 k_1}{s(A_1 + A_2) + A_1 k_2 + A_2 k_1} \tag{A3}$$

Rearranging gives

$$\begin{aligned} \frac{\alpha s + (\beta + \alpha\gamma)}{s + \gamma} = &\left[\frac{s(B_1 + B_2)}{(A_1 + A_2)}\right. \\ &\left. + \frac{B_1 k_2 + B_2 \mathrm{N} k_1}{(A_1 + A_2)}\right] \Big/ \left[s + \frac{A_1 k_2 + A_2 k_1}{(A_1 + A_2)}\right] \end{aligned} \tag{A4}$$

The relationships between the α, β, and γ terms and the A, B, and k terms can be derived readily from (A4) since both sides of (A4) are in the same general form $\left(\frac{as + b}{s + c}\right)$:

$$\alpha = \frac{B_1 + B_2}{A_1 + A_2} \tag{A5}$$

$$\gamma = \frac{A_1 k_2 + A_2 k_1}{A_1 + A_2} \tag{A6}$$

$$\beta + \alpha\gamma = \frac{B_1 k_2 + B_2 k_1}{A_1 + A_2} \tag{A7}$$

and by substitution of (A5) and (A6) into (A7), we obtain

$$\beta = \frac{(A_1 + A_2)(B_1 k_2 + B_2 k_1) - (B_1 + B_2)(A_1 k_2 + A_2 k_1)}{(A_1 + A_2)^2} \tag{A8}$$

Thus, for the simple case of $n = 2$, analytical relationships between the α, β, and γ terms and the A_i and B_i terms exist.

$n = 3$

Again, from Eq. (A2),

$$\begin{aligned} &\frac{\beta_1}{s + \gamma_1} + \frac{\beta_2}{s + \gamma_2} + \alpha \\ &\quad = \left(\frac{B_1}{s + k_1} + \frac{B_2}{s + k_2} + \frac{B_3}{s + k_3}\right) \Big/ \\ &\qquad \left(\frac{A_1}{s + k_1} + \frac{A_2}{s + k_2} + \frac{A_3}{s + k_3}\right) \end{aligned} \tag{A9}$$

the two sides of which can be rearranged to give

$$\Rightarrow \frac{\alpha s^2 + [\alpha(\gamma_1 + \gamma_2) + \beta_1 + \beta_2]s + \gamma_1\beta_2 + \gamma_2\beta_1 + \alpha\gamma_1\gamma_2}{s^2 + s(\gamma_1 + \gamma_2) + \gamma_1\gamma_2} =$$

$$\left\{\frac{s^2(B_1 + B_2 + B_3)}{(A_1 + A_2 + A_3)}\right.$$

$$\left. + \frac{s[B_1(k_2 + k_3) + B_2(k_1 + k_3) + B_3(k_1 + k_2)]}{(A_1 + A_2 + A_3)}\right.$$

$$+ \frac{B_1k_2k_3 + B_2k_1k_3 + B_3k_1k_2}{(A_1 + A_2 + A_3)}\Big\} \Big/ \quad \text{(A10)}$$

$$\Big\{s^2 + \frac{s[A_1(k_2 + k_3) + A_2(k_1 + k_3) + A_3(k_1 + k_2)]}{(A_1 + A_2 + A_3)}$$

$$+ \frac{A_1k_2k_3 + A_2k_1k_3 + A_3k_1k_2}{(A_1 + A_2 + A_3)}\Big\}$$

While far more laborious and less physically applicable, the relationships between the α, β, and γ terms and the A, B, and k terms can be derived in a fashion analogous to that used for $n = 2$, since both sides of (A10) are in the same general form as one another $(as^2 + bs + c)/(s^2 + ds + e)$:

$$\alpha = \frac{B_1 + B_2 + B_3}{A_1 + A_2 + A_3} \quad \text{[A11]}$$

Also, from (A10) it is seen that by solving the following two expressions simultaneously, terms for γ_1 and γ_2 can be obtained:

$$\gamma_1 + \gamma_2 = \frac{[A_1(k_2 + k_3) + A_2(k_1 + k_3) + A_3(k_1 + k_2)]}{(A_1 + A_2 + A_3)} \quad \text{(A12)}$$

$$\gamma_1\gamma_2 = \frac{A_1k_2k_3 + A_2k_1k_3 + A_3k_1k_2}{(A_1 + A_2 + A_3)}$$

The terms for γ_1 and γ_2 are actually given by the two roots of the following quadratic equation (A13):

$$\gamma^2 - \gamma\frac{[A_1(k_2 + k_3) + A_2(k_1 + k_3) + A_3(k_1 + k_2)]}{[A_1 + A_2 + A_3]} \quad \text{(A13)}$$

$$+ \frac{[A_1k_2k_3 + A_2k_1k_3 + A_3k_2k_1]}{[A_1 + A_2 + A_3]} = 0$$

$$\gamma_{1(2)} = \frac{\left(X \pm \sqrt{(-X)^2 - 4(A_1 + A_2 + A_3)(A_1k_2k_3 + A_2k_1k_3 + A_3k_1k_2)}\right)}{\left(2(A_1 + A_2 + A_3)\right)} \quad \text{(A14)}$$

where

$$X = A_1k_2 + A_1k_3 + A_2k_1 + A_2k_3 + A_3k_1 + A_3k_2$$

Note that γ_1 and γ_2 are dependent on k_i and A_i only, i.e., they are independent of B_1, B_2, and B_3. Note, also, that γ_1 and γ_2 are independent of the magnitudes of A_1, A_2, and A_3 and depend only on the *relative* magnitudes.

Similarly, from (A10) it is seen that by solving the following two expressions simultaneously, terms for β_1 and β_2 can be obtained:

$$\alpha\gamma_1\gamma_2 + \gamma_1\beta_2 + \gamma_2\beta_1 = \frac{[B_1k_2k_3 + B_2k_1k_3 + B_3k_1k_2]}{(A_1 + A_2 + A_3)} \quad \text{(A15)}$$

$$\alpha(\gamma_1 + \gamma_2) + \beta_1 + \beta_2 = \frac{[B_1(k_2 + k_3) + B_2(k_1 + k_3) + B_3(k_1 + k_2)]}{(A_1 + A_2 + A_3)}$$

While these equations can be solved for β_1 and β_2, the solutions are even more unwieldy than (A14) but can be solved numerically.

ACKNOWLEDGMENTS

Discussions with Drs. Jon Morgan, Ben Crystall, and Linda Swanson are gratefully acknowledged.

REFERENCES

1. D. V. O'Connor and D. Phillips (1983) *Time-Correlated Single Photon Counting*, Academic Press, New York.
2. M. C. Chang, S. H. Courtney, A. J. Cross, R. J. Gulotty, J. W. Petrich, and G. R. Fleming (1985) *Anal. Inst.* **14**, 433–464.
3. C. Lewis, W. R. Ware, L. J. Doemeny, and T. L. Nemzek (1973) *Rev. Sci. Instrum.* **44**, 107–114.
4. P. Wahl, J. C. Auchet, and B. Donzel (1974) *Rev. Sci. Instrum.* **45**, 28–32.
5. D. M. Rayner, A. E. McKinnon, A. G. Szabo, and P. A. Hackett (1976) *Can. J. Chem.* **54**, 3246–3259.
6. R. W. Wijnaendts van Resandt, R. H. Vogel, and S. W. Provencher (1982) *Rev. Sci. Instrum.* **53**, 1392–1397.
7. J.-E. Löfroth (1985) *Eur. Biophys. J.* **13**, 45–58.
8. G. Rumbles, A. J. Brown, and D. Phillips (1991) *J. Chem. Soc. Faraday Trans.* **87**, 825–830.
9. J. R. Lakowicz and A. Balter (1982) *Biophys. Chem.* **15**, 353–360.
10. J. R. Lakowicz and A. Balter (1982) *Biophys. Chem.* **16**, 223–240.
11. M. Hauser and G. Wagenblast (1983) in R. B. Cundall and R. E. Dale (Eds.), *Time-Resolved Fluorescence Spectroscopy in Biochemistry and Biology*, Plenum Press, New York, pp. 463–480.
12. J. Vogelsang and M. Hauser (1990) *J. Phys. Chem.* **94**, 7488–7494.
13. M. D. Barkley, A. A. Kowalczyk, and L. Brand (1981) *J. Chem. Phys.* **75**, 3581–3593.
14. D. J. S. Birch and R. E. Imhof (1991) in J. R. Lakowicz (Ed.), *Topics in Fluorescence Spectroscopy*, Plenum Press, New York, Vol. 1, pp. 1–95.
15. J. M. Beechem, E. Gratton, M. Ameloot, J. R. Knutson, and L. Brand (1989) *The Global Analysis of Fluorescence Intensity and Anisotropy Decay Data: Second Generation Theory and Programs*, Laboratory for Fluorescence Dynamics, Department of Physics, University of Illinois at Urbana–Champaign.
16. J. M. Beechem, E. Gratton, M. Ameloot, J. R. Knutson, and L. Brand (1991) in J. R. Lakowicz (Ed.), *Topics in Fluorescence Spectroscopy*, Plenum Press, London, Vol. 2, pp. 241–305.
17. A. E. McKinnon, A. G. Szabo, and D. R. Miller (1977) *J. Phys. Chem.* **81**, 1564–1570.
18. D. V. O'Connor, W. R. Ware, and J. C. Andre (1979) *J. Phys. Chem.* **83**, 1333–1343.

19. H. P. Good, A. J. Kallır, and U. P. Wild (1984) *J. Phys. Chem.* **88**, 5435–5441.
20. D. W. Marquardt (1963) *J. Soc. Ind. Appl. Math* **11**, 431–441.
21. P. R. Bevington (1969) *Data Reduction and Error Analysis for the Physical Sciences*, McGraw–Hill, New York.
22. A. Grinvald and I. Z. Steinberg (1974) *Anal. Biochem.* **59**, 583–598.
23. A. E. W. Knight and B. K. Selinger (1971) *Spectrochim. Acta* **27A**, 1223–1234.
24. A. E. W. Knight and B. K. Selinger (1973) *Aust. J. Chem.* **26**, 1–27.
25. T. Murao, I. Yamazakı, and K. Yoshihara (1982) *Appl. Opt.* **21**, 2297–2298.
26. G. Rumbles, T. A. Smith, I. Soutar, and L. Swanson (in press).
27. A. J. Marsh, G. Rumbles, I. Soutar, and L. Swanson (1992) *Chem. Phys. Lett.* **195**, 31–35.
28. A. J. Cross and G. R. Fleming (1984) *Biophys. J.* **46**, 45–56.
29. R. L. Christensen, R. C. Drake, and D. Phillips (1986) *J Phys. Chem.* **90**, 5960–5967.
30. J. B. Birks, D. J. Dyson, and I. H. Munro (1963) *Proc. Roy. Soc. Lond.* **A275**, 575–588.
31. D. Phillips, A. J. Roberts, and I. Soutar (1980) *J Polym. Sci. Polym. Lett. Ed.* **18**, 123–129.
32. D. A. Holden, P. Y.-K. Wang, and J. E. Guillet (1980) *Macromolecules* **13**, 295–298.
33. T. A. Smith, G. D. Scholes, G. O. Turner, and K. P. Ghiggino (1994) *J. Chem. Soc. Faraday Trans.* **90**, 2845–2847.
34. T. A. Smith, D. A. Shipp, G. D. Scholes, and K. P. Ghiggino (1994) *J. Photochem. Photobiol. A* **80**, 177–185.